Experimental observation of ragged synchronizability

P. Perlikowski, B. Jagiello, A. Stefanski, and T. Kapitaniak
Division of Dynamics, Technical University of Lodz, Stefanowskiego 1/15, 90-924 Lodz, Poland
(Received 29 January 2008; revised manuscript received 12 May 2008; published 31 July 2008)

Synchronization thresholds of an array of nondiagonally coupled oscillators are investigated. We present experimental results which show the existence of ragged synchronizability, i.e., the existence of multiple disconnected synchronization regions in the coupling parameter space. This phenomenon has been observed in an electronic implementation of an array of nondiagonally coupled van der Pol's oscillators. Numerical simulations show good agreement with the experimental observations.

DOI: 10.1103/PhysRevE.78.017203 PACS number(s): 05.45.Xt, 05.45.Pq, 07.50.Ek

Synchronization [1] has become a well-known and widely used feature in driven periodic and chaotic oscillators. Over the last decade the subject of network synchronization has attracted increasing attention from different fields [1–7]. Synchronization thresholds and their dependence on various structural parameters of the network, such as the type and strength of coupling [2] are of particular interest. The introduction of the master stability function (MSF) [3] allowed for the establishment of a number of important results [4,5].

In our previous work [6], we presented an example of nondiagonally coupled array of Duffing oscillators, in which multiple disconnected synchronous regions of coupling strength occur. The term nondiagonal coupling means that the network nodes are linked with others via nondiagonal components of linking (output) function [see Eq. (5)]. We have also observed the appearance or disappearance of such synchronous windows in coupling parameter space, when the number of oscillators in the array or topology of connections between them changes. This phenomenon has been called the ragged synchronizability (RSA). The existence of RSA has been numerically confirmed in [7].

In this Brief Report we give the experimental evidence of the existence of RSA. We consider the dynamics of an array of coupled van der Pol's (VdP) oscillators which has been implemented as an electronic circuit. Our numerical studies are supported by a simple electronic experiment. Our experimental results are in satisfactory agreement with numerical simulations.

In our experimental and numerical studies, the VdP oscillator

$$\dot{x} = z,$$

$$\dot{z} = d(1 - x^2)z - x + \cos(\eta\tau), \tag{1}$$

where d and η are constant, has been taken as an array node. η represents the frequency of the external excitation. Consider an open array of three coupled VdP oscillators shown in Fig. 1. The evolution of oscillators coupled in this array is given by

$$\dot{x}_1 = z_1, \tag{2a}$$

$$\dot{z}_1 = d(1 - x_1^2)z_1 - x_1 + \cos(\eta\tau) + \sigma(2x_2 - 2x_1), \tag{2b}$$

$$\dot{x}_2 = z_2, \tag{2c}$$

$$\dot{z}_2 = d(1 - x_2^2)z_2 - x_2 + \cos(\eta\tau) + \sigma(2x_1 + x_3 - 3x_2), \tag{2d}$$

$$\dot{x}_3 = z_3, \tag{2e}$$

$$\dot{z}_3 = d(1 - x_3^2)z_3 - x_3 + \cos(\eta\tau) + \sigma(x_2 - x_3), \tag{2f}$$

where σ is a constant coupling coefficient.

In numerical analysis we assume $d=0.401$, $\eta=1.207$, and consider σ as a control parameter. In experiments we use an electronic implementation of this array shown in Fig. 2.

The dynamics of the considered array can be described in a block form,

$$\dot{\mathbf{x}} = \mathbf{F}(\mathbf{x}) + (\sigma\mathbf{G} \otimes \mathbf{H})\mathbf{x}, \tag{3}$$

where $\mathbf{x}=(\mathbf{x}_1,\mathbf{x}_2,\mathbf{x}_3) \in \mathbb{R}^6$, $\mathbf{F}(x)=[\mathbf{f}(\mathbf{x}_1),\mathbf{f}(\mathbf{x}_2),\mathbf{f}(\mathbf{x}_3)]$, $\mathbf{G}$ is the connectivity matrix, i.e., the Laplacian matrix representing the topology of connections between the network nodes,

$$\mathbf{G} = \begin{bmatrix} -2 & 2 & 0 \\ 2 & -3 & 1 \\ 0 & 1 & -1 \end{bmatrix}, \tag{4}$$

$\otimes$ is a direct (Kronecker) product of two matrices and $\mathbf{H}:\mathbb{R}^2 \to \mathbb{R}^2$ is an output function of each oscillator's variables that is used in the coupling (it is the same for all nodes). The connection of oscillators shown in Eqs. (2a)–(2f) can be classified as a case of pure (diagonal components are equal to zero) nondiagonal coupling due to the form of output function

$$\mathbf{H} = \begin{bmatrix} 0 & 0 \\ 1 & 0 \end{bmatrix}. \tag{5}$$

Here, a subject of our interest are the ranges of the coupling coefficient σ where the so-called complete synchronization, i.e., full coincidence of phases (frequencies) and amplitudes of responses of coupled systems [1], occurs. The complete synchronization requires an ideal identity of these systems,

FIG. 1. The model of an open array of van der Pol's oscillators (VdPO).

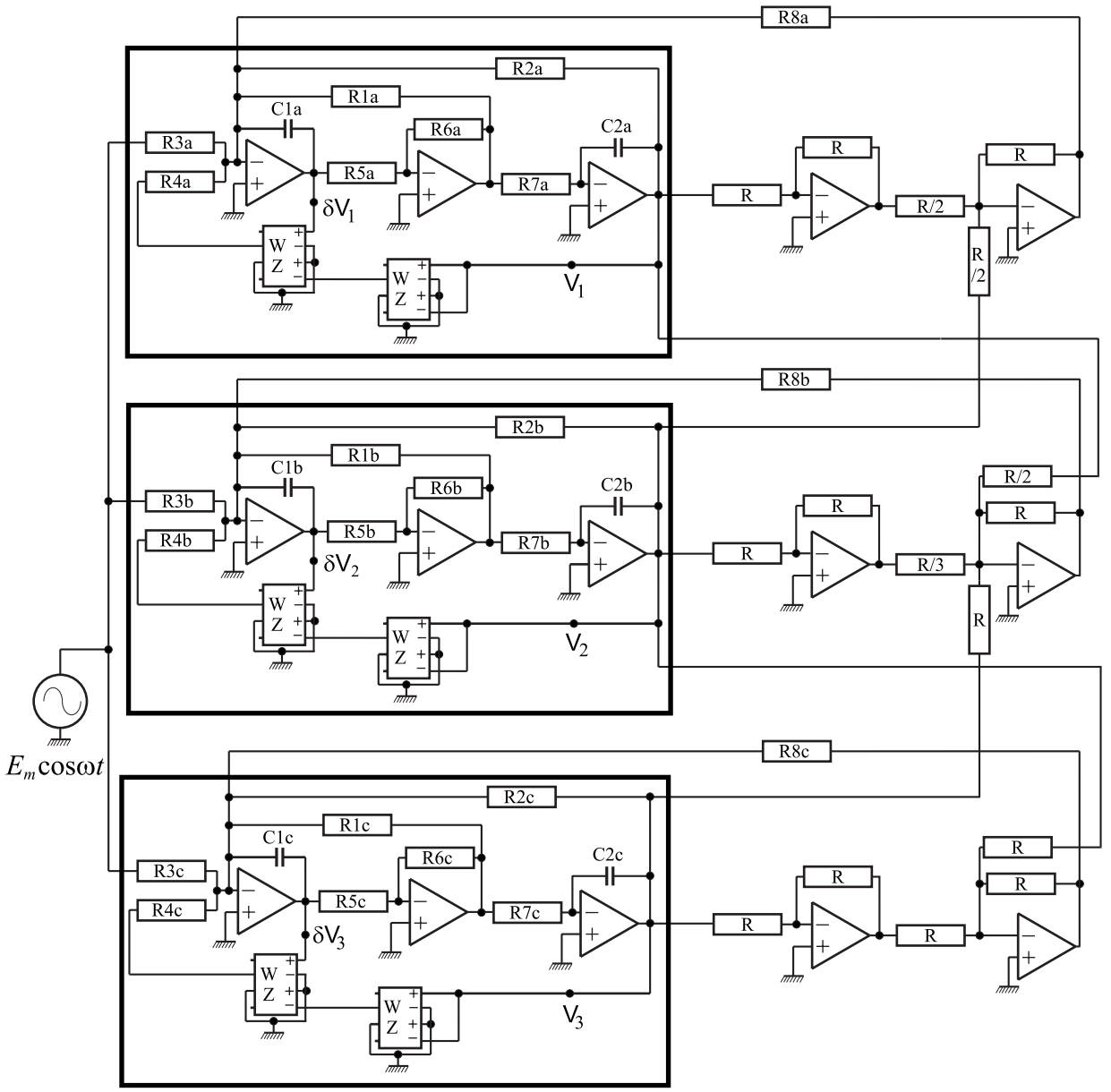

FIG. 2. An electronic implementation of an open array of VdP oscillators shown in Fig. 1.

i.e., they are given with the same ordinary differential equations with identical system's parameters. In order to estimate the synchronization thresholds of coupling parameter, we apply the idea of the MSF [3]. Under this approach, the synchronizability of a network of oscillators can be quantified with eigenvalues γ_k of connectivity matrix $\mathbf{G}$, $k=0,1,2$. In the case under consideration, matrix $\mathbf{G}$ has three real eigenvalues $\gamma_0=0$, $\gamma_1=-1.27$, $\gamma_2=-4.73$, so this is a variant of diffusive real coupling [4] (in the general case γ_k can be a complex number). After the block diagonalization of the variational equation of Eq. (3) there appear three separated blocks $\dot{\xi}_k=[D\mathbf{f}+\sigma\gamma_k D\mathbf{H}]\xi_k$, where $D\mathbf{f}$ and $D\mathbf{H}$ are Jacobi matrices of the node system and linking function, respectively ($k=1,2,3$). For $\gamma_0=0$ we have linearized the equation of the node system [Eq. (1)] which is corresponding to the mode longitudinal to invariant synchronization manifold $\mathbf{x}_1=\mathbf{x}_2=\mathbf{x}_3$. The remaining two eigenvalues $\gamma_{1,2}$ represent two different transverse modes of perturbation from synchronous state [3,4].

Assuming that γ represents an arbitrary value of γ_k and ξ symbolizes an arbitrary transverse mode, we can define the generic variational equation for any node system

$$\dot{\xi}=[D\mathbf{f}+\sigma\gamma D\mathbf{H}]\xi. \tag{6}$$

Substituting the analyzed system [Eq. (1)] in Eq. (6) we obtain

$$\dot{\xi}=\zeta,$$

$$\dot{\zeta}=d(1-x^2)\zeta-2dx\xi z-\xi+\sigma\gamma\xi. \tag{7}$$

Thus, the generic variational equation [Eq. (7)] describes an evolution of any perturbation in the directions transversal to the final synchronous state, that dynamics is governed by

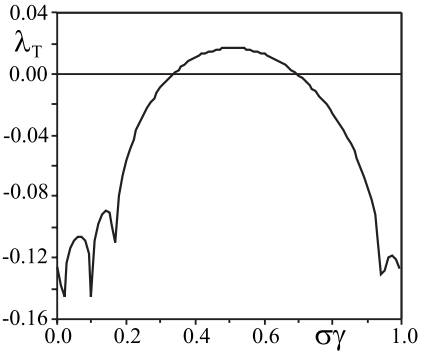

FIG. 3. The largest transversal Lyapunov exponent λ_T, calculated for generic variational equation (7), versus product $\sigma\gamma$; $\eta=1.207$, $d=0.401$.

Eq. (1). Now, we can define the MSF for the considered case as a bifurcational diagram of the largest transversal Lyapunov exponent λ_T, calculated for the generic variational equation [Eq. (7)], versus product $\sigma\gamma$. The MSF graph for the presented example [Eqs. (1) and (7)] is depicted in Fig. 3. If products $\sigma\gamma_{1,2}$ corresponding to both transversal eigenmodes (in the general case any number of them) can be found in the ranges of negative transversal Lyapunov exponent, then the synchronous state is stable for the analyzed configuration of couplings.

In order to confirm our numerical simulations experimentally we have built a setup which is schematically depicted in Fig. 2. Each VdP oscillator has been implemented as the circuit [8] (shown in black frame in Fig. 2) composed of two capacitors $C1$ and $C2$, seven resistors $R(1-7)$, and two multiplicators AD-633JN which introduce nonlinearity. Multiplicators have the following characteristic: $W=(1/V_c)(X_1-X_2)(Y_1-Y_2)+Z$, where X_1, X_2, Y_1, and Y_2 are the input signals, W is an output signal, and $V_c=10$ V is a characteristic voltage. The input $E_m \cos \omega t$, where amplitude E_m and frequency ω are constant, represents external excitation. The additional resistors $R8$ and R have been used to realize the coupling. In our implementation we used out of shelf elements: $R1=9920[\Omega]$, $R2=999[\Omega]$, $R3=501[\Omega]$, $R4=100[\Omega]$, $R5=10\,000[\Omega]$, $R6=10\,000[\Omega]$, $R7=16\,150[\Omega]$, $R=180\,000[\Omega]$, $C1=10[nF]$, $C2=10[nF]$. $R8 \in [0\Omega, 44\,000\Omega]$ has been taken as a control parameter. The equivalent elements in each circuit can differ by 1% of their nominal values.

The relation between the circuits real parameters and dimensionless parameters of Eqs. (2a)–(2f) is as follows: $\omega_0^2=\frac{1}{C1C2R2R7}$, $d=\frac{1}{C1R1\omega_0}$, $\eta=\frac{\omega}{\omega_0}$, $x_{1-3}=V_{1-3}\frac{R3}{E_mR2}$, $z_{1-3}=\delta V_{1-3}\frac{R3}{E_mR2\omega_0}$, $\sigma=\frac{R2}{R8}$. Nonidentity of elements used in each circuit introduces the mismatches of d and σ parameters in Eqs. (2b), (2d), and (2f). The estimated mismatches are smaller than ± 0.001.

Data acquisition is performed using a Data Acquisition System 3200A\415 board connected to a computer controlled by software developed in Microstar Labs. The dynamical variables of interest in this circuit are the voltages V_{1-3} of each oscillator measured in the points indicated in Fig. 2. The first derivatives of the potentials δV_{1-3} are taken in the point also indicated in Fig. 2.

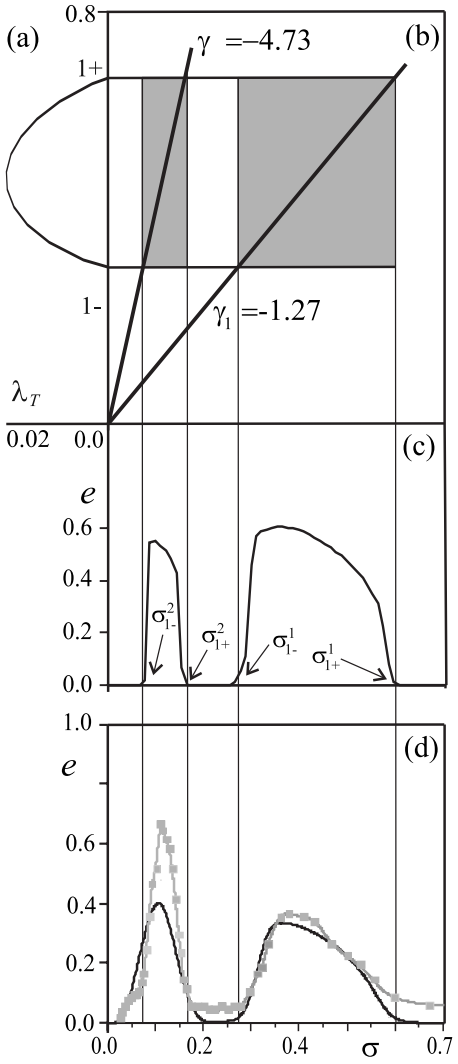

FIG. 4. Comparison of numerical and experimental results, $d=0.401$, $\eta=1.207$; (a)–(c) desynchronizing mechanism: A projection from the MSF diagram (a), via eigenvalues γ_k of connectivity matrix $\mathbf{G}$ (b), to the bifurcation diagram of synchronization error e versus coupling coefficient σ (c) (desynchronous intervals are shown in gray, complete synchronization takes place in σ ranges where e approaches zero value), (d) synchronization error e versus σ; experimental results, gray line with scatters (marking measurement points), numerical results for the case of parameter mismatch; black line, the values of d taken in Eqs. (2b), (2d), and (2f) are, respectively, 0.400, 0.401, and 0.402.

In our example we have considered $\eta=1.207$ and its real equivalent $\omega=4780$ Hz in experiment. Then, in the absence of coupling each oscillator exhibits periodic behavior (the largest LE $\lambda_1=-0.126$) with the period equal to the period of excitation. Looking at the MSF diagram (Fig. 3), we can expect an appearance of the RSA of coupled VdP oscillators [Eq. (1)], because two disconnected regions of negative transversal Lyapunov exponent $[\sigma\gamma \in (0,1-)$ or $(1+,\infty)]$ can be observed. Consequently, at least two separated synchronous ranges of coupling parameter σ should be visible, i.e., the RSA effect takes place. However, synchronous intervals of the coefficient σ not always are an exact reflection of the MSF intervals, where the transversal Lyapunov exponent

is positive. The RSA mechanism is explained in Figs. 4(a)–4(c), where a projection from the MSF diagram [Fig. 4(a)], via eigenvalues of connectivity matrix **G** [Fig. 4(b)], to the bifurcation diagram of synchronization error

$$e = \sum_{i=2}^{3} |(x_1 - x_i)|, \tag{8}$$

versus coupling strength σ [Fig. 4(c)] is shown. Complete synchronization takes place in the σ ranges where e approaches zero value [Fig. 4(c)]. We can observe third synchronous $(\sigma^2_{1+}, \sigma^1_{1-})$ and second desynchronous $(\sigma^2_{1-}, \sigma^2_{1+})$ σ intervals in comparison with only two synchronous and one desynchronous MSF ranges, respectively. "Additional" desynchronous interval appears because the mode 2 (associated with eigenvalue γ_2) crosses the desynchronous MSF interval $(1-,1+)$ while the mode 1 (associated with γ_1) is still located in the first synchronous MSF interval $(0,1-)$, see Fig. 4(b). Then in the narrow range $(\sigma^2_{1+}, \sigma^1_{1-})$, two modes are in synchronous MSF interval so that one can observe an "additional window" of synchronization in the σ interval. The second desynchronous σ interval corresponds to mode 1 desynchronizing bifurcation. Finally, the steady synchronous state is achieved due to increasing coupling strength at $\sigma = 0.6$. The ragged synchronizability manifests in alternately appearing windows of synchronization and desynchronization. In the above description some special notation for σ ranges has been introduced. Such a notation brings information of which mode (first or second) desynchronizing bifurcation (superscripts) takes place during the transition from the synchronous to the desynchronous regime and which edge of the desynchronous interval of MSF (1− and 1+ in subscripts correspond to lower and higher edges, respectively) is associated with the given boundary value of the coupling coefficient. In Fig. 4(d) the results of experimental investigation of the synchronization process in the analyzed circuit are demonstrated. The plot of experimentally generated synchronization error [reduced to nondimensional form and calculated with the use of Eq. (8)] versus coupling strength σ is shown in gray with scatters. Obviously, in the case of real VdP oscillators the perfect complete synchronization cannot be achieved due to unavoidable parameter mismatch. However, in such a case the imperfect complete synchronization can be observed, i.e., the correlation of amplitudes and phases of the system's responses is not ideal, but a synchronization error remains relatively small during the time evolution. One can notice a qualitative coincidence between numerical simulations and experiment comparing Fig. 4(c) with Fig. 4(d), i.e., regions of the imperfect complete synchronization tendency in a real circuit correspond well to the complete synchronization ranges in a numerical model. In the last stage of our research the influence of parameters mismatch on the synchronization error e has been analyzed numerically. We have estimated a slight disparity of the values of d in all three VdP oscillators with measuring their real parameters. Next, such an approximated mismatch has been realized in the considered model [Eqs. (2a)–(2f)] [the values of d taken in Eqs. (2b), (2d), and (2f) are, respectively, 0.400, 0.401, and 0.402]. The synchronization error simulated numerically for this model is represented with a black line in Fig. 4(d). Its good visible agreement with experimental result shows that a slight difference of coupled oscillators does not destroy their synchronization tendency, i.e., the imperfect complete synchronization takes place.

To summarize, comparing analytical (obtained by MSF approach) [Fig. 4(b)], numerical [Fig. 4(c)], and experimental results [Fig. 4(d)] we can confirm the occurrence of the RSA in the real system of coupled oscillators. We have observed this phenomenon in an electronic implementation of an array of VdP oscillators with nondiagonal coupling between the nodes. A good agreement between numerical simulation and experimental observations which shows that the mechanism responsible for the appearance or disappearance of the windows of synchronizability is the same as described in [6]. It seems that the phenomenon of RSA is common for the systems with nondiagonal coupling and not sensitive for the small parameter mismatch, i.e., can be observed in real experimental systems.

This work has been supported by the Polish Department for Scientific Research (DBN) under Contracts No. 4 T07A 044 28 and No. 0710/B/TO2/2007/33.

[1] H. Fujisaka and T. Yamada, Prog. Theor. Phys. **69**, 32 (1983); V. S. Afraimovich, N. N. Verichev, and M. Rabinovich, Radiofiz. **28**, 1050 (1985); I. Blekhman, *Synchronization in Science and Technology* (ASME Press, New York, 1988); L. M. Pecora and T. L. Carroll, Phys. Rev. Lett. **64**, 821 (1990); A. Pikovsky, M. Rosenblum, and J. Kurths, *Synchronization. A Universal Concept in Nonlinear Sciences* (Cambridge University Press, Cambridge, UK, 2001); S. Boccaletti, J. Kurths, D. Osipov, D. L. Valladares, and C. S. Zhou, Phys. Rep. **366**, 1 (1990).

[2] T. Yamada and H. Fujisaka, Prog. Theor. Phys. **70**, 1240 (1983); A. Pikovsky, Z. Phys. B: Condens. Matter **55**, 149 (1984); A. Stefanski, J. Wojewoda, T. Kapitaniak, and S. Yanchuk, Phys. Rev. E **70**, 026217 (2004); S. Dmitriev, M. Shirokov, and S. O. Starkov, IEEE Trans. Circuits Syst., I: Fundam. Theory Appl. **44**, 918 (1997).

[3] L. M. Pecora and T. L. Carroll, Phys. Rev. Lett. **80**, 2109 (1998); L. M. Pecora, Phys. Rev. E **58**, 347 (1998).

[4] L. M. Pecora, T. L. Carroll, G. Johnson, D. Mar, and K. Fink, Int. J. Bifurcation Chaos Appl. Sci. Eng. **10**, 273 (2000); K. Fink, G. Johnson, T. L. Carroll, D. Mar, and L. M. Pecora, Phys. Rev. E **61**, 5080 (2000).

[5] M. Barahona and L. M. Pecora, Phys. Rev. Lett. **89**, 054101 (2002); T. Nishikawa, A. E. Motter, Y.-C. Lai, and F. C. Hoppensteadt, *ibid.* **91**, 014101 (2003).

[6] A. Stefanski, P. Perlikowski, and T. Kapitaniak, Phys. Rev. E **75**, 016210 (2007).

[7] M. Zhao, G. R. Chen, T. Zhou, and B.-H. Wang, Fron. Phys. China **2**, 46 (2007); Z. Duan, G.-R. Chen, and L. Huang, e-print arXiv:0706.2901v1; W. Zou and M. Zhan, Europhys. Lett. **81**, 10006 (2008).

[8] B. Nana and P. Woafo, Phys. Rev. E **74**, 046213 (2006).